Available online at www.sciencedirect.com
ScienceDirect
Physics Letters B 659 (2008) 297–307
PHYSICS LETTERS B
www.elsevier.com/locate/physletb

Triple Higgs boson production in the linear collider

Giancarlo Ferrera [a], Jaume Guasch [b,c], David López-Val [a], Joan Solà [a,c,*]

[a] *High Energy Physics Group, Departament ECM, Universitat de Barcelona, Av. Diagonal 647, E-08028 Barcelona, Catalonia, Spain*
[b] *Gravitation and Cosmology Group, Departament FF, Universitat de Barcelona, Av. Diagonal 647, E-08028 Barcelona, Catalonia, Spain*
[c] *Institut de Ciències del Cosmos, Universitat de Barcelona, Barcelona, Spain*

Received 3 August 2007; received in revised form 15 October 2007; accepted 19 October 2007

Available online 12 November 2007

Editor: A. Ringwald

Abstract

Triple Higgs boson production (3H) may provide essential information to reconstruct the Higgs potential. We consider 3H-production in the International Linear Collider (ILC) both in the Minimal Supersymmetric Standard Model (MSSM) and in the general Two-Higgs-Doublet Model (2HDM). We compute the total cross-section for the various 3H final states, such as $H^+H^-h^0$, $H^0A^0h^0$, etc., and compare with the more traditional double Higgs (2H) boson production processes. While the cross-sections for the 2H final states lie within the same order of magnitude in both the MSSM and 2HDM, we find that for the 3H states the maximum 2HDM cross-sections, being of order 0.1 pb, are much larger than the MSSM ones which, in most cases, are of order 10^{-6} pb or less. Actually, the 3H processes could be the dominant mechanism for Higgs boson production in the 2HDM. Ultimately, the origin of the remarkable enhancement of the 3H channels in the 2HDM case (for both type I and type II models) originates in the structure of the trilinear Higgs boson couplings. The extremely clean environment of the ILC should allow a relatively comfortable tagging of the three Higgs boson events. In view of the fact that the MSSM contribution is negligible, these events should manifest themselves mainly in the form of 6 heavy-quark jet final states. Some of these signatures could be spectacular, and in case of being detected would constitute strong evidence of an extended Higgs sector of non-supersymmetric origin.

PACS: 95.36.+x; 04.62.+v; 11.10.Hi

1. Introduction

There is no doubt that the Higgs sector is the most paradigmatic one in the structure of any modern quantum field theory (QFT) aiming at a good phenomenological description of electroweak interactions in particle physics. The main reason for this is twofold: (i) the Higgs mechanism is the only known consistent quantum field theoretical procedure to generate masses for all the elementary particles; (ii) we have found no Higgs boson yet—not even the single one predicted by the successful standard model (SM) of the strong and electroweak interactions—and therefore we do not know if Higgs bosons exist at all or if, on the contrary, there are extensions of the SM containing a richer spectrum of Higgs boson particles, some of them electrically charged and some of them electrically neutral. Let us note that if failure of point (ii) would persist for long, especially after the LHC and the future linear colliders ILC and/or CLIC had already amply swept their maximum energy ranges and luminosities, we could find ourselves in a sort of *cul-de-sac* because this would also mean that we would not have substantiated point (i) either, which is tantamount to say that we would have not found any experimental evidence of the most powerful theoretical mechanism known up to date for building renormalizable models of particle interactions. It is therefore a momentous task to search for Higgs bosons and unveil their ultimate nature.

Surely a linear e^+e^- collider will be instrumental to accomplish this aim because it is the cleanest high-precision machine

* Corresponding author at: High Energy Physics Group, Departament ECM, Universitat de Barcelona, Av. Diagonal 647, E-08028 Barcelona, Catalonia, Spain.
E-mail addresses: ferrera@ecm.ub.es (G. Ferrera), jaume.guasch@ub.edu (J. Guasch), dlopez@ecm.ub.es (D. López-Val), sola@ifae.es (J. Solà).

0370-2693/$ – see front matter
doi:10.1016/j.physletb.2007.10.072

we can think of for studying particle interactions. No doubt, if Higgs bosons are around, the linear collider will help either to discover them or to identify the precise nature of the Higgs particle(s) previously uncovered at the LHC. In particular, once a neutral Higgs boson has been identified, we would like to know if it is the neutral SM Higgs boson, or if it belongs to some supersymmetric (SUSY) extension of the SM, or if on the contrary it has nothing at all to do with SUSY. If, alternatively, the identified Higgs boson is charged we would like to know to which extension of the SM it can be ascribed. A particularly well-motivated possibility along these lines is the Minimal Supersymmetric Standard Model (MSSM) [1]. But another, simpler, one is just the general (unconstrained) Two-Higgs-Doublet Model (2HDM) [2].

Double Higgs boson (2H) production in a linear collider has been investigated in great detail in the literature, although mainly in the MSSM [3–5]. Such process cannot proceed in the SM at the tree-level, so we know that if we would detect a sizeable rate of 2H final states in a e^+e^- collider it would be an unmistakable sign of physics beyond the SM. However, a tree-level analysis of these pairwise-produced unconventional Higgs bosons is most likely insufficient to unravel their true nature. Therefore, a dedicated work on radiative correction calculations has been undertaken. A rich literature exists indeed on the one-loop calculation of the cross-sections for the two-particle final states

$$e^+e^- \to 2H \quad \left(2H \equiv h^0A^0; H^0A^0; H^+H^-\right), \tag{1.1}$$

essentially in the MSSM case.[1] Similarly, the two-body final states $e^+e^- \to Zh$ and $e^+e^- \to Ah$ (with $h = h^0H^0$) are long known to be complementary to each other in the MSSM [3]. There are also studies considering radiative corrections to charged Higgs production in e^+e^- collisions within the 2HDM [10], and double and multiple Higgs production at the LHC [11], but to our knowledge a complete analysis of the processes (1.1) in the general 2HDM is lacking [12].

In another vein, triple Higgs boson (3H) production may open new vistas in our desperate hunting for the mass generation mechanism. These processes can be very important because they carry essential information to reconstruct the Higgs boson potential and thus of the Higgs mechanism itself. The Higgs potential of any renormalizable QFT may contain in general mass terms, trilinear Higgs boson self-interactions and quartic self-interactions. For instance, the trilinear coupling HHH has been investigated phenomenologically in TeV-class linear colliders in Refs. [4,7,8] through the double Higgs strahlung process $e^+e^- \to HHZ$ or the WW double Higgs fusion mechanism $e^+e^- \to H^+H^-\nu_e\bar{\nu}_e$. These processes involve vertices like ZZH, WWH, ZZHH, WWHH and HHH, and are possible both in the SM and in extensions of the SM, like the MSSM and the general 2HDM. Unfortunately the cross-section turns out to be rather small (of order of a fb at most) both in the SM and in the MSSM [7]. Even worse is the situation with the triple Higgs boson production in the MSSM, unless in some specific configuration of the parameter space with resonant enhancement of the signal, see Section 3. Out of the resonance, the typical cross-sections are of order of 0.01 fb or less [7]. In the previous reference it has been shown that if the double and triple Higgs production cross-sections would yield sufficiently high signal rates, the system of couplings and corresponding double/triple Higgs production cross-sections could be solved for all trilinear Higgs self-couplings up to discrete ambiguities, by using these processes. However, in practice the cross-sections are too small to be all measurable.

In this Letter we wish to study the trilinear coupling HHH in the general 2HDM case by focusing on exclusive triple Higgs boson final states produced at the ILC. We find that there are scenarios where the HHH coupling could actually be identified relatively easily. This is because in the general 2HDM it can be highly enhanced as compared to the MSSM case (which is purely gauge). To show the phenomenological impact of this enhancement, and also to briefly compare with the MSSM situation, we compute the 3H production cross-sections for all possible $\mathcal{CP}$-conserving final states both in the MSSM and the 2HDM. The seven allowed triple Higgs boson channels can be sorted out in three main classes:

$$\begin{aligned} &(1)\quad e^+e^- \to H^+H^-h, \qquad (2)\quad e^+e^- \to hhA^0, \\ &(3)\quad e^+e^- \to h^0H^0A^0 \quad \left(h = h^0, H^0, A^0\right), \end{aligned} \tag{1.2}$$

where in class (2) we understand that the two neutral Higgs bosons h must be the same, i.e. the allowed final states are $(hhA^0) = (h^0h^0A^0)$, $(H^0H^0A^0)$ and $(A^0A^0A^0)$. We show that the 2HDM cross-sections can be several orders of magnitude larger than the corresponding MSSM ones. Interestingly enough, the 3H cross-sections can be comparable and even significantly larger than the 2H cross-sections irrespective of the latter being computed in the MSSM or in the 2HDM.

2. General 2HDM: Relevant interactions and restrictions

In this section we shall briefly present the interactions and phenomenological restrictions relevant to our calculation. Let us recall that the general 2HDM is obtained by canonically extending the SM Higgs sector with a second $SU_L(2)$ doublet with weak hypercharge $Y = 1$, so that it contains 4 complex scalar fields arranged as follows:

$$\begin{aligned} \Phi_1 &= \begin{pmatrix} \Phi_1^+ \\ \Phi_1^0 \end{pmatrix} \quad (Y = +1), \\ \Phi_2 &= \begin{pmatrix} \Phi_2^+ \\ \Phi_2^0 \end{pmatrix} \quad (Y = +1). \end{aligned} \tag{2.1}$$

In the supersymmetric case, in order to construct a consistent superpotential [1] one replaces Φ_1 with the conjugate ($Y = -1$) $SU_L(2)$ doublet

$$H_1 = \begin{pmatrix} H_1^0 \\ H_1^- \end{pmatrix} \equiv \epsilon\Phi_1^* = \begin{pmatrix} \Phi_1^{0*} \\ -\Phi_1^- \end{pmatrix} \quad (Y = -1). \tag{2.2}$$

Here $\epsilon = i\sigma_2$. For simplicity we stick to the canonical form (2.1) because we need not presume SUSY, the correspondence with the MSSM case being now clear ($\Phi_1 = -\epsilon H_1^*$).

[1] See [6–8], and also the extensive report [9] and references therein.

In this framework the most general structure of the $\mathcal{CP}$-conserving, gauge invariant, renormalizable Higgs potential preserving the discrete symmetry $\Phi_i \to (-1)^i \Phi_i$ $(i = 1, 2)$, reads [2]:

$$\begin{aligned} V(\Phi_1, \Phi_2) = {} & \lambda_1 \big(\Phi_1^\dagger \Phi_1 - v_1^2\big)^2 + \lambda_2 \big(\Phi_2^\dagger \Phi_2 - v_2^2\big)^2 \\ & + \lambda_3 \big[\big(\Phi_1^\dagger \Phi_1 - v_1^2\big) + \big(\Phi_2^\dagger \Phi_2 - v_2^2\big)\big]^2 \\ & + \lambda_4 \big[\big(\Phi_1^\dagger \Phi_1\big)\big(\Phi_2^\dagger \Phi_2\big) - \big(\Phi_1^\dagger \Phi_2\big)\big(\Phi_2^\dagger \Phi_1\big)\big] \\ & + \lambda_5 \big[\mathrm{Re}\big(\Phi_1^\dagger \Phi_2\big) - v_1 v_2\big]^2 + \lambda_6 \big[\mathrm{Im}\big(\Phi_1^\dagger \Phi_2\big)\big]^2, \end{aligned} \tag{2.3}$$

λ_i $(i = 1, \ldots, 6)$ being dimensionless real parameters. Once the neutral components of the Higgs doublets acquire non-vanishing VEVs (vacuum expectation values), the electroweak (EW) symmetry $SU_L(2) \times U_Y(1)$ breaks down to $U(1)_{em}$, in such a way that we can obtain the physical spectrum of the Higgs sector upon diagonalization of Eq. (2.3). We are thus left with two $\mathcal{CP}$-even Higgs bosons h^0, H^0, a $\mathcal{CP}$-odd Higgs boson A^0 and a pair of charged Higgs bosons $\mathrm{H}^\pm$. The free parameters in the general 2HDM are usually chosen to be as follows: the masses of the physical Higgs particles (M_{h^0}, M_{H^0}, M_{A^0}, $M_{\mathrm{H}^\pm}$); the ratio of the two VEVs $\langle H_i^0 \rangle \equiv v_i/\sqrt{2}$ $(i = 1, 2)$ giving masses to the up- and down-like quarks,

$$\tan\beta \equiv \frac{\langle H_2^0 \rangle}{\langle H_1^0 \rangle} \equiv \frac{v_2}{v_1}; \tag{2.4}$$

the mixing angle α between the two $\mathcal{CP}$-even states; and finally the coupling λ_5, which cannot be absorbed in the previous quantities and becomes tied to the structure of the Higgs self-couplings. In total, we have 7 free parameters, which indeed correspond to the original 6 couplings λ_i and the two VEVs v_1, v_2—the latter being submitted to the physical constraint $v^2 \equiv v_1^2 + v_2^2 = G_F^{-1}/\sqrt{2}$, where G_F is Fermi's constant (equivalently, $v^2 = 4M_{\mathrm{W}}^2/g^2$, where M_{W} is the $\mathrm{W}^\pm$ mass and g the $SU_L(2)$ gauge coupling constant). Incidentally, let us note that the essential parameter (2.4) could be ideally measured in $\mathrm{e}^+\mathrm{e}^-$ colliders [5] e.g. through production and decay of $\mathrm{H}^\pm$ or A^0 since in these cases the rates do not involve the mixing angle α. It is also worth noticing that two of the λ_i parameters can be directly related to physical Higgs boson masses and to the Fermi constant: $\lambda_4 = 2M_{\mathrm{H}^\pm}^2/v^2 = 2\sqrt{2}G_F M_{\mathrm{H}^\pm}^2$ and $\lambda_6 = 2M_{\mathrm{A}^0}^2/v^2 = 2\sqrt{2}G_F M_{\mathrm{A}^0}^2$. These relations are valid only at the tree level.

Let us point out that the aforementioned discrete symmetry imposed on (2.3), which is only softly violated by the dimension-two terms, is necessary to ensure the absence of tree-level flavor changing neutral currents (FCNC). It is well known that this discrete symmetry is automatically preserved in the MSSM. However in the general case it has to be imposed, and then two main scenarios arise [2]: (1) In the so-called type I 2HDM one Higgs doublet (Φ_2) couples to all of the SM fermions, whereas the other one (Φ_1) does not couple to them at all; (2) In contrast, in the type II 2HDM the doublet Φ_1 (respectively Φ_2) couples only to down-like (respectively up-like) quarks. In the latter case, an additional discrete symmetry in the chiral components of the fermion sector, namely $f_i \to (-1)^i f_i$ (for left- and right-handed fields $i = 1, 2$, respectively), must be imposed in order to banish the tree-level FCNC processes. Let us recall that the MSSM Higgs sector is a type II one of a very restricted sort (it is enforced to be SUSY invariant) [1,2]. We shall not dwell here on the Higgs boson interactions with fermions (see [2] for details) because they are not involved in any of our tree-level Higgs boson production processes (1.1)–(1.2). Let us finally recall that SUSY invariance of the potential introduces 5 constraints that reduce the number of free parameters to 2, usually taken to be M_{A^0} and $\tan\beta$ [2]. In particular, SUSY enforces that the two terms softly breaking the discrete symmetry of the potential must be equal: $\lambda_5 = \lambda_6 = 2\sqrt{2}G_F M_{\mathrm{A}^0}^2$. For simplicity, and in order to keep closer to the MSSM structure of the Higgs sector, sometimes one adopts this setting [13]. We will follow this practice and therefore the final number of free parameters in our analysis will be 6. They can be arranged as follows:

$$(M_{\mathrm{h}^0}, M_{\mathrm{H}^0}, M_{\mathrm{A}^0}, M_{\mathrm{H}^\pm}, \tan\alpha, \tan\beta). \tag{2.5}$$

Essential for our calculation are the trilinear Higgs couplings. These are not explicitly present in Eq. (2.3), but they are generated after spontaneous breaking of the EW symmetry. In the SM the trilinear and quartic Higgs couplings have fixed values, which uniquely depend on the actual mass of the Higgs boson. In the case of the MSSM, and due to the SUSY invariance, the Higgs self-couplings are of pure gauge nature [2]. This is in fact the reason for the tiny triple Higgs boson production rates obtained for the processes (1.2) within the framework of the MSSM [7], see Section 3. In contrast, the general 2HDM accommodates trilinear Higgs couplings with great potential enhancement. In Table 1 we list those entering our computations, in a form already accommodating the condition $\lambda_5 = \lambda_6$. These couplings are written in terms of the physical fields and Goldstone bosons, which are obtained after rotating the electroweak eigenstates (2.1) into the physical mass-eigenstates by means of the two diagonalization angles α and β. As can be seen, the couplings in Table 1 depend on the 6 free parameters (2.5). The behavior and enhancement capabilities of these Higgs boson self-interactions are at the heart of our calculation of the cross-sections (1.2) within the general 2HDM (type I and type II).

However, an important point when studying possible sources of unconventional physics is to ensure that the SM behavior is sufficiently well reproduced up to the energies explored so far. Such a requirement translates into a number of constraints over the parameter space of the given model. In particular, this severely limits the a priori enhancement possibilities of the Higgs boson self-interactions in the 2HDM. First of all we have to keep the theory within a perturbative regime, which entails that only values in the approximate range $0.1 \lesssim \tan\beta \lesssim 60$ shall be allowed. Also very important is to maintain the so-called (approximate) $SU(2)$ custodial symmetry [14]. In models of physics beyond the SM this is done in terms of the parameter ρ, which defines the ratio of the neutral to charged current Fermi constants. In general it takes the form $\rho = \rho_0 + \delta\rho$, where ρ_0 is the tree-level value. In any model containing an arbitrary number of doublets (in particular the 2HDM), we have

Table 1
Trilinear Higgs boson self-interactions in the Feynman gauge within the 2HDM. Here G^0 is the neutral Goldstone boson. These vertices are involved in the Feynman diagrams of Fig. 1 in Section 3. Vertices with gauge bosons are common with the MSSM and are not included, see [2]

$H^\pm H^\mp H^0$	$-\frac{ie}{M_W \sin\theta_W \sin 2\beta}[(M^2_{H^\pm} - M^2_{A^0} + \frac{1}{2}M^2_{H^0})\sin 2\beta\cos(\beta-\alpha) - (M^2_{H^0} - M^2_{A^0})\cos 2\beta \sin(\beta-\alpha)]$
$H^\pm H^\mp h^0$	$-\frac{ie}{M_W \sin\theta_W \sin 2\beta}[(M^2_{H^\pm} - M^2_{A^0} + \frac{1}{2}M^2_{h^0})\sin 2\beta\sin(\beta-\alpha) + (M^2_{h^0} - M^2_{A^0})\cos 2\beta \cos(\beta-\alpha)]$
$h^0 h^0 H^0$	$-\frac{ie\cos(\beta-\alpha)}{2M_W \sin\theta_W \sin 2\beta}[(2M^2_{h^0} + M^2_{H^0})\sin 2\alpha - M^2_{A^0}(3\sin 2\alpha - \sin 2\beta)]$
$h^0 H^0 H^0$	$\frac{ie\sin(\beta-\alpha)}{2M_W \sin\theta_W \sin 2\beta}[(M^2_{h^0} + 2M^2_{H^0})\sin 2\alpha - M^2_{A^0}(3\sin 2\alpha - \sin 2\beta)]$
$A^0 A^0 H^0$	$-\frac{ie}{2M_W \sin\theta_W \sin 2\beta}[M^2_{H^0}\sin 2\beta\cos(\beta-\alpha) - 2(M^2_{H^0} - M^2_{A^0})\cos 2\beta\sin(\beta-\alpha)]$
$A^0 A^0 h^0$	$-\frac{ie}{2M_W \sin\theta_W \sin 2\beta}[M^2_{h^0}\sin 2\beta\sin(\beta-\alpha) + 2(M^2_{h^0} - M^2_{A^0})\cos 2\beta\cos(\beta-\alpha)]$
$h^0 h^0 h^0$	$-\frac{3ie}{M_W \sin\theta_W \sin 2\beta}[M^2_{h^0}[\cos(\beta+\alpha) + \frac{1}{2}\sin 2\alpha\sin(\beta-\alpha)] - M^2_{A^0}\cos^2(\beta-\alpha)\cos(\beta+\alpha)]$
$H^0 H^0 H^0$	$-\frac{3ie}{M_W \sin\theta_W \sin 2\beta}[M^2_{H^0}[\sin(\beta+\alpha) - \frac{1}{2}\sin 2\alpha\cos(\beta-\alpha)] - M^2_{A^0}\sin^2(\beta-\alpha)\sin(\beta+\alpha)]$
$G^0 H^0 A^0$	$\frac{ie}{2M_W \sin\theta_W \sin 2\beta}\sin(\beta-\alpha)[M^2_{H^0} - M^2_{A^0}]$
$G^0 h^0 A^0$	$-\frac{ie}{2M_W \sin\theta_W \sin 2\beta}\cos(\beta-\alpha)[M^2_{h^0} - M^2_{A^0}]$

$\rho_0 = M_W^2/M_Z^2\cos^2\theta_W = 1$, and then $\delta\rho$ represents the deviations from 1 induced by pure quantum corrections. From the known SM contribution and the experimental constraints [15] we must enforce that the additional quantum effects coming from 2HDM dynamics ought to satisfy $|\delta\rho_{2HDM}| \leqslant 10^{-3}$. It is thus important to stay in a region of parameter space where this bound is respected. Let us recall that the 2HDM one-loop contribution is given by [16]

$$\begin{aligned}\delta\rho_{2HDM} = \frac{G_F}{8\sqrt{2}\pi^2}\Bigg\{ & M^2_{H^\pm}\Bigg[1 - \frac{M^2_{A^0}}{M^2_{H^\pm} - M^2_{A^0}}\ln\frac{M^2_{H^\pm}}{M^2_{A^0}}\Bigg] \\ & + \cos^2(\beta-\alpha)M^2_{h^0}\Bigg[\frac{M^2_{A^0}}{M^2_{A^0} - M^2_{h^0}}\ln\frac{M^2_{A^0}}{M^2_{h^0}} \\ & - \frac{M^2_{H^\pm}}{M^2_{H^\pm} - M^2_{h^0}}\ln\frac{M^2_{H^\pm}}{M^2_{h^0}}\Bigg] \\ & + \sin^2(\beta-\alpha)M^2_{H^0}\Bigg[\frac{M^2_{A^0}}{M^2_{A^0} - M^2_{H^0}}\ln\frac{M^2_{A^0}}{M^2_{H^0}} \\ & - \frac{M^2_{H^\pm}}{M^2_{H^\pm} - M^2_{H^0}}\ln\frac{M^2_{H^\pm}}{M^2_{H^0}}\Bigg]\Bigg\}. \end{aligned} \tag{2.6}$$

From this expression it is clear that if $M_{A^0} \to M_{H^\pm}$ then $\delta\rho_{2HDM} \to 0$, and hence if the mass splitting between M_{A^0} and $M_{H^\pm}$ is not significant $\delta\rho_{2HDM}$ can be kept within bounds.

Also remarkable are the restrictions over the charged Higgs masses coming from FCNC radiative B-meson decays, whose branching ratio $\mathcal{B}(b \to s\gamma) \simeq 3 \times 10^{-4}$ [15] is measured with sufficient precision to be sensitive to new physics. The (charged) Higgs boson contribution to the aforementioned decay is positive and increases when $M_{H^\pm}$ decreases. An averaged bound of $M_{H^\pm} > 350$ GeV for $\tan\beta \geqslant 1$ ensues from [17]. It must be recalled that this bound does not apply to type I models since for them the charged Higgs couplings to fermions are proportional to $\cot\beta$ and hence the loop contributions are highly suppressed at large $\tan\beta$. By the same token too light charged Higgs boson contributions are also restricted at very low $\tan\beta \ll 1$ for both type I and type II models.

Apart from these restrictions, and of course respecting the general Higgs boson mass bounds obtained from unsuccessful searches at LEP [15], we must consider also the unitarity bounds. Such bounds come from the fact that the trilinear 2HDM couplings, hereafter denoted $C(HHH)$, can receive very large enhancements at high $\tan\beta$. Although unitarity limits can be presented in a rather detailed and cumbersome way, we shall avoid cluttering and proceed as in [13]. Therefore, to assess that the 2HDM remains unitary, we will adhere to the practice of bounding the size of the 2HDM trilinear Higgs boson couplings by the value of their single SM counterpart $\lambda^{(SM)}_{HHH}$ at the scale of 1 TeV:

$$\begin{aligned}\big|C(HHH)\big| &\leqslant \big|\lambda^{(SM)}_{HHH}(M_H = 1\text{ TeV})\big| \\ &= \frac{3eM_H^2}{2\sin\theta_W M_W}\bigg|_{M_H = 1\text{ TeV}}, \end{aligned} \tag{2.7}$$

where $-e$ is the electron charge and θ_W is the weak mixing angle. The range of Higgs boson masses and other 2HDM parameters ensuing from this condition fall in the ballpark of the more complete set of (tree-level) unitarity conditions formulated in various sophisticated—albeit non-fully coincident—ways in the literature [18].

3. Triple Higgs boson production: Numerical analysis

Throughout the present work we have made use of the standard algebraic and numerical packages *FeynArts*, *FormCalc* and *LoopTools* [19] for the obtention of the Feynman diagrams, the analytical computation and simplification of the scattering amplitudes and the numerical evaluation of the cross-section. Feynman diagrams for the tree-level Higgs-pair production (2H) processes are very simple and are not shown here, whereas a sample of typical Feynman diagrams for the triple (3H) Higgs boson production processes is displayed in Fig. 1. Let us first concentrate on the 2H final states in the general 2HDM. As in-

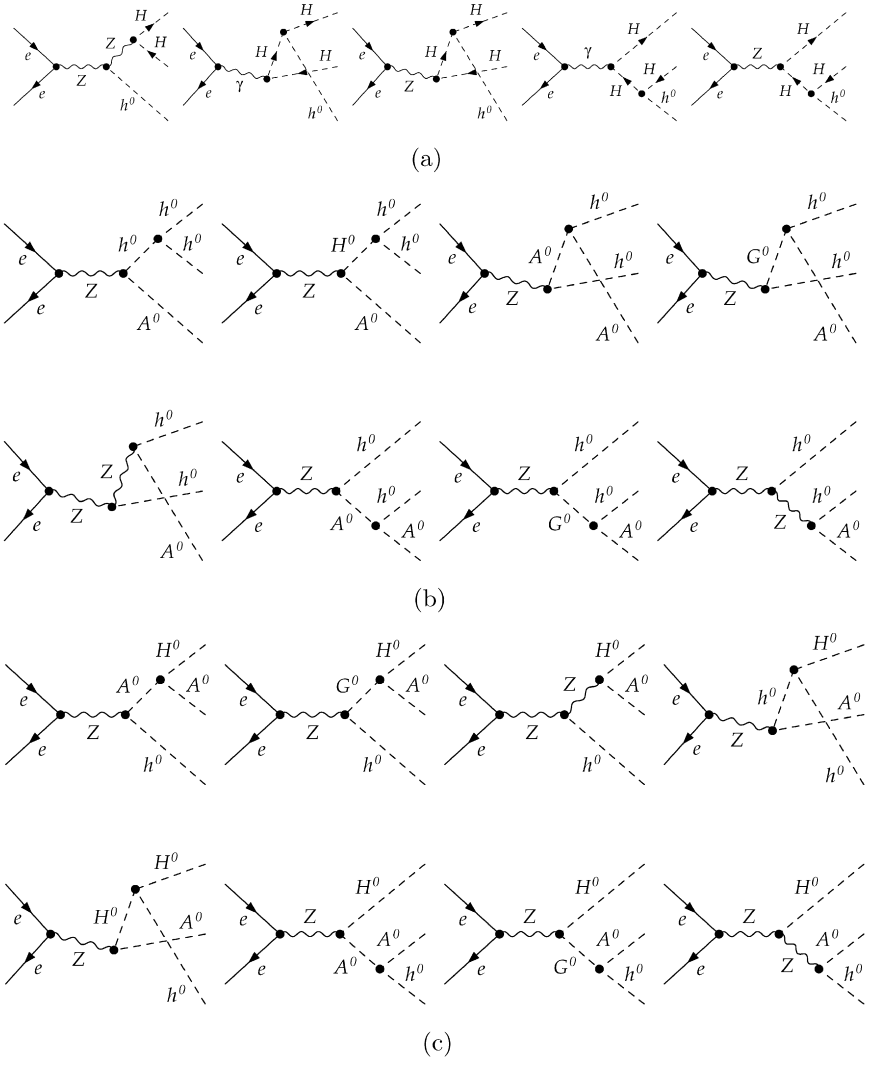

Fig. 1. Tree-level Feynman diagrams corresponding to three of the triple Higgs boson production processes indicated in Eq. (1.2). The other four processes proceed through similar collections of diagrams.

dicated in the introduction, these are well studied in the MSSM case. Here we shall report first on the tree-level results for 2H production in both the MSSM and general 2HDM, mainly to compare with the triple Higgs boson channels which are indeed the main aim of the present study.

It is not our intention to present here the one-loop analysis of the 2H processes within the general 2HDM, except to briefly report on those which can only work at the one-loop level.[2] For instance, due to $\mathcal{CP}$-conservation (even more: due to Bose–Einstein statistics), some of the possible channels (namely $e^+e \to h^0h^0$, $e^+e \to H^0H^0$, $e^+e \to A^0A^0$) are forbidden at the tree level and can take place only through 1-loop box-type diagrams. We have evaluated the corresponding cross-sections and turn out to be in the range of 10^{-5} pb (that is to say, they entail around 1 event only per 100 fb^{-1} of integrated luminosity), a too minute rate to provide feasible detection signals. Notice that in the SM these tree-level forbidden processes are induced by the same set of box diagrams, and consequently the SM rates are of the same order. Quite another is the situation with the other channels, Eq. (1.1), which are $\mathcal{CP}$-allowed at the tree-level and hence furnish sizeable rates. Since only couplings of the guise Higgs–Higgs-gauge boson play a role, the interactions are of purely gauge nature and do not differ from the general 2HDM to the MSSM [2]. Therefore, we expect both models to provide similar cross-sections for all the processes (1.1). For the numerical evaluation of the 2H cross-sections, we have to input specific values for the free 2HDM parameters defined in Section 2, see Eq. (2.5). On the one hand, we will set the mixing angles α, β in such a way that the aforementioned Higgs–Higgs-gauge boson couplings are optimized. This can be easily done, for instance by setting $\alpha = \beta$ in $e^+e \to h^0A^0$, in which case the relevant coupling $C(A^0h^0Z^0) \sim \cos(\beta - \alpha)$ is maximum. In Fig. 2 we plot the total cross-section σ (in pb) as a function of the center-of-mass energy $\sqrt{s}$ (in GeV) for the different channels (1.1). We explore two different regimes: (a) light Higgs masses and (b) heavy Higgs masses. To represent these regimes we use in this case Sets I and III of Higgs

[2] For details of the full one-loop analysis, see [12].

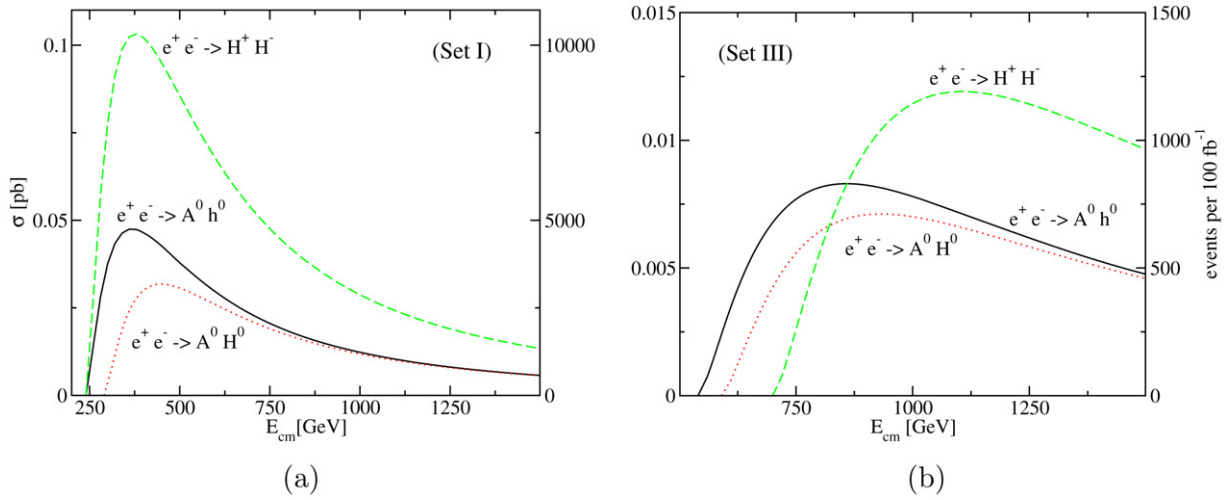

Fig. 2. Total cross-section σ (in pb) and number of events per 100 fb^{-1} as a function of $E_{cm} = \sqrt{s}$ for the tree-level Higgs boson pair production channels (1.1) in the general 2HDM within two regimes of masses: (a) *light* Higgs bosons and (b) *heavy* Higgs bosons, represented by the mass Sets I and III respectively in Table 2.

Table 2
Sets I, II and III of *light* and *heavy* Higgs boson masses in the 2HDM. Sets I and III are used for 2H production in Fig. 2, and Sets II and III for 3H production in Fig. 3 and 4

	Set I	Set II	Set III
M_{h^0} (GeV)	100	100	200
$M_{H^\pm}$ (GeV)	120	120	350
M_{H^0} (GeV)	150	150	250
M_{A^0} (GeV)	140	300	340

Table 3
Maximum cross-sections (in pb) for the 2H production channels within the MSSM at $\sqrt{s} = 1$ TeV

	σ_{max} ($\sqrt{s} = 1$ TeV)	M_{A^0} (GeV)	$\tan\beta$
$e^+e \to A^0h^0$	0.013	100	60
$e^+e \to A^0H^0$	0.012	130	60
$e^+e \to H^+H^-$	0.028	100	5.5

boson masses in Table 2. Sets I and II differ only in the $\mathcal{CP}$-odd Higgs mass, M_{A^0}, which is substantially lighter in the former as compared to the latter. Indeed, we wish to use Set I for the study of 2H production in order not to artificially suppress it by mere phase space reasons. On the other hand, Set II (together with Set III) will be used later on for the study of 3H production. From Fig. 2(a) we see that in the light Higgs boson mass regime the production rates are substantial, attaining in all cases a few thousands events per 100 fb^{-1} of integrated luminosity, with maximum values reaching $\sigma(e^+e^- \to H^+H^-) \sim 0.1$ pb. For heavy Higgs bosons, Fig. 2(b) tells us that the achieved production rates are around one order of magnitude below. Nevertheless, even in these less favored scenarios the predicted rates are still quite sizeable within the clean ILC environment.

It is of course of interest to contrast the above 2H results with the predicted contributions in the MSSM case, see Table 3. Recall from Section 2 that the MSSM Higgs sector is fully determined (at the tree-level) by a pair of free parameters, namely $\tan\beta$ and M_{A^0}. Taking advantage of this simple structure of the parameter space, we have systematically searched for the values of $(\tan\beta,\ M_{A^0})$ such that the cross-section at fixed $\sqrt{s} = 1$ TeV becomes optimal while simultaneously fulfilling all the phenomenological constraints on the SUSY Higgs masses. Notice that in the MSSM the charged Higgs boson mass is not so severely restricted as in the case of the general 2HDM models of type II (see Section 2) because the squark and chargino contributions to $\mathcal{B}(b \to s\gamma)$ can compensate for the charged Higgs effects [17]. A default set of MSSM parameters (quoted in Table 4) has been employed to compute the Higgs boson masses. These include the quantum effects obtained from the standard code provided by the computational tool package [19], which implements the results of Ref. [20]. We remark that M_{SUSY} in Table 4 stands for a common value of the LL and RR soft SUSY-breaking masses in the squark mass matrices. To be sure, the numerical search for the maximum of $\sigma(2H)$ for the processes (1.1) has been made under the condition that m_{h^0} is larger than its lower experimental bound (~ 90 GeV [15]). Let us also note that, in order to get more accurate results, a running value for the electromagnetic coupling constant $\alpha(M_Z) = 1/127.9$ has been used. All in all, the (approximate) optimal values obtained for 2H production within the MSSM are summarized in Table 3. We see that the predicted cross-sections are of the order of 10^{-2} pb and, as anticipated, they are comparable to the 2HDM values for similar masses. Therefore, sizeable rates of non-standard Higgs-pair production can be achieved at the ILC for both SUSY and non-SUSY extended Higgs sectors, and in this sense the two models are difficult to distinguish using the 2H channels. As mentioned

Table 4
Choice of parameters used for the computation of 2H and 3H production in the MSSM

M_{SUSY} (GeV)	1000
μ (GeV)	200
A_t (GeV)	1000
A_b (GeV)	1000
A_τ (GeV)	1000

in the introduction, a clear separation between the two models can only be accomplished through the detailed study of radiative corrections to 2H production in both the MSSM [6] and the 2HDM [12].

Let us now discuss the case of the triple Higgs boson production in e^+e^- annihilations within the general 2HDM. The processes under consideration are those in Eq. (1.2). Again we wish to compute the cross-sections for them and compare with the corresponding MSSM values. As far as the 2HDM is concerned, we shall keep making use of two separate regimes of masses, light and heavy, but in this case they will be represented by Sets II and III respectively in Table 2. Actually, due to the low energy $b \to s\gamma$ constraint (mentioned in Section 2) on the charged Higgs boson mass in type II models, we cannot keep the $\mathcal{CP}$-odd mass M_{A^0} relatively light (as in Set I) for these models. The distinction between the two sets of masses (Sets II and III) is thus necessary. Set II accommodates higher values of M_{A^0} than Set I, but only Set III reflects a mass region allowed in type II 2HDM. In fact, due to the constraint $|\delta\rho_{2\mathrm{HDM}}| < 10^{-3}$—cf. Eq. (2.6)—it turns out that not only $M_{H^\pm}$, but also M_{A^0}, must necessarily be heavier in type II models.

The Feynman diagrams for the most prominent triple Higgs boson processes (1.2) are depicted in Fig. 1. We can see that they involve trilinear Higgs boson couplings of the form indicated in Table 1. Let us illustrate the origin of the potential enhancement inherent to these couplings by just focusing on one of them, for example the first one, $C(H^\pm H^\pm H^0)$. One can easily check that for $\tan\beta \gg 1$ or $\tan\beta \ll 1$ and $\alpha \simeq 0$, the coupling grows effectively as $\sim \tan\beta$ or $\sim \cot\beta$, respectively. Therefore, the corresponding cross-section can be significantly enhanced by a factor $\tan^2\beta$ or $\cot^2\beta$, respectively. We will mainly explore the enhancement in the large $\tan\beta$ region, which is more natural and also more efficient. An additional enhancement source in $C(H^\pm H^\pm H^0)$ is the possible mass splittings between the Higgs boson masses, e.g. between $M^2_{A^0}$ and $M^2_{H^0}$, which is also subdued in part by the $\delta\rho_{2\mathrm{HDM}}$ constraint mentioned above. In contrast to this situation, in the MSSM the triple Higgs couplings do not have any such enhancements. Indeed, in the MSSM the (tree-level) analogous of the coupling under consideration is

$$C_{\mathrm{MSSM}}\big(H^\pm H^\pm H^0\big) = \frac{-ieM_W}{\sin\theta_W}\left[\cos(\beta-\alpha) - \frac{\cos 2\beta\cos(\alpha+\beta)}{2\cos^2\theta_W}\right]. \tag{3.1}$$

It is patent that there is no source of enhancement, the coupling being gauge-like. In general the Higgs boson self-couplings in the MSSM undergo radiative corrections [21] (as the Higgs boson masses themselves), but in practice the 3H cross-sections remain rather small [4,7,8]. In contrast, the enhancement effect of the general 2HDM trilinear couplings, listed in Table 1, can have a much bigger impact on the cross-sections while respecting all known bounds. In this respect, we recall that these couplings can also receive radiative corrections in the general 2HDM [22]. However, we do not include them here because our main goal is to show that the 3H production signal can be significantly enhanced in the general 2HDM, and for this it suffices to confine ourselves to the tree-level structure. More refined studies of this signal may be necessary in the future, in which case the inclusion of corrections should be appropriate.

We have plotted the 3H cross-sections for the general 2HDM in Figs. 3 and 4 for the Higgs boson mass Sets II and III in Table 2. We see that they can reach the level of ~ 0.1 pb or more, therefore implying promising rates of at least 10^4 events per 100 fb^{-1} of integrated luminosity. The larger cross-sections are obtained considering light Higgs masses (Set II of Table 2). This is because there is a lower suppression of the final phase-space and also because the maximum of the cross-section is reached at lower energies $\sqrt{s} \sim$ (700–1000) GeV. Furthermore, as expected, all the cross-sections are seen to increase approximately as $\tan^2\beta$ due to the behavior of the trilinear couplings. In the heavy Higgs boson scenario (Set III), the maximum is shifted to higher values $\sqrt{s} \sim 1500$ GeV. Taking into account the presence of the Z boson propagator, the cross-section scales with the energy and thus the corresponding maximum becomes between one to two orders of magnitude smaller than in the light Higgs boson scenario. These results for Set III (adequate to type II models) translate into rates of $\mathcal{O}(10^2$–$10^3)$ events per 100 fb^{-1} of integrated luminosity, which should still allow comfortable detection of the signal. As for the remaining Higgs production channels (not considered in our figures), they provide smaller values of the maximum cross-section: e.g. those with final states $H^+H^-A^0$ and $H^0H^0A^0$ yield maximum cross-sections of order 10^{-2} pb for Set II and $(10^{-3}$–$10^{-4})$ pb for Set III. Finally, channel $A^0A^0A^0$ is a rather inconspicuous one due to the phase-space suppression and also to the fact that we have three identical particles in the final state (hence an additional suppression of 1/3!), leaving maximum cross-sections of order 10^{-4} pb and 10^{-5} pb for Sets II and III at $\sqrt{s} = 1400$ GeV.

Some technical details are now in order. To find the values of the angles α and β that generate the maximum of the cross-section $\sigma_{\max}(3H)$ for the various 3H processes we have performed a systematic scan using the Sets II and III of parameters given in Table 2 under the restrictions mentioned in Section 2. The result is that in all cases the largest possible values of $\tan\beta$ are preferred rather than intermediate or very small ones. However, $\tan\beta$ cannot be arbitrarily large (or arbitrarily small), not only due to the perturbative bound, but also because of the unitarity constraint. For this reason in Figs. 3 and 4 we have limited ourselves to plot the cross-sections for a few values of $\tan\beta$ up to $\tan\beta = 40$. We have already exemplified how some trilinear couplings are maximized e.g. for large $\tan\beta$ and $\alpha \simeq 0$, but others are not so enhanced in this region. Our numerical scan shows that the following intermediate strategy optimizes the cross-sections: once $\tan\beta$ is chosen at the largest allowed value, we choose $\alpha = \pi/2 - \beta - \delta$, typically with $\delta = 0.8$ (rad.). This is enough to circumvent the unitarity and perturbative restriction and get the optimal set of cross-sections. These are the ones studied in Figs. 3 and 4. Let us also point out that the maximum in each process is not severely peaked; we have verified that there is a large region of parameter space (including $\alpha \simeq \beta$) where the cross-sections are still perfectly sizeable (within the same order of magnitude as $\sigma_{\max}$).

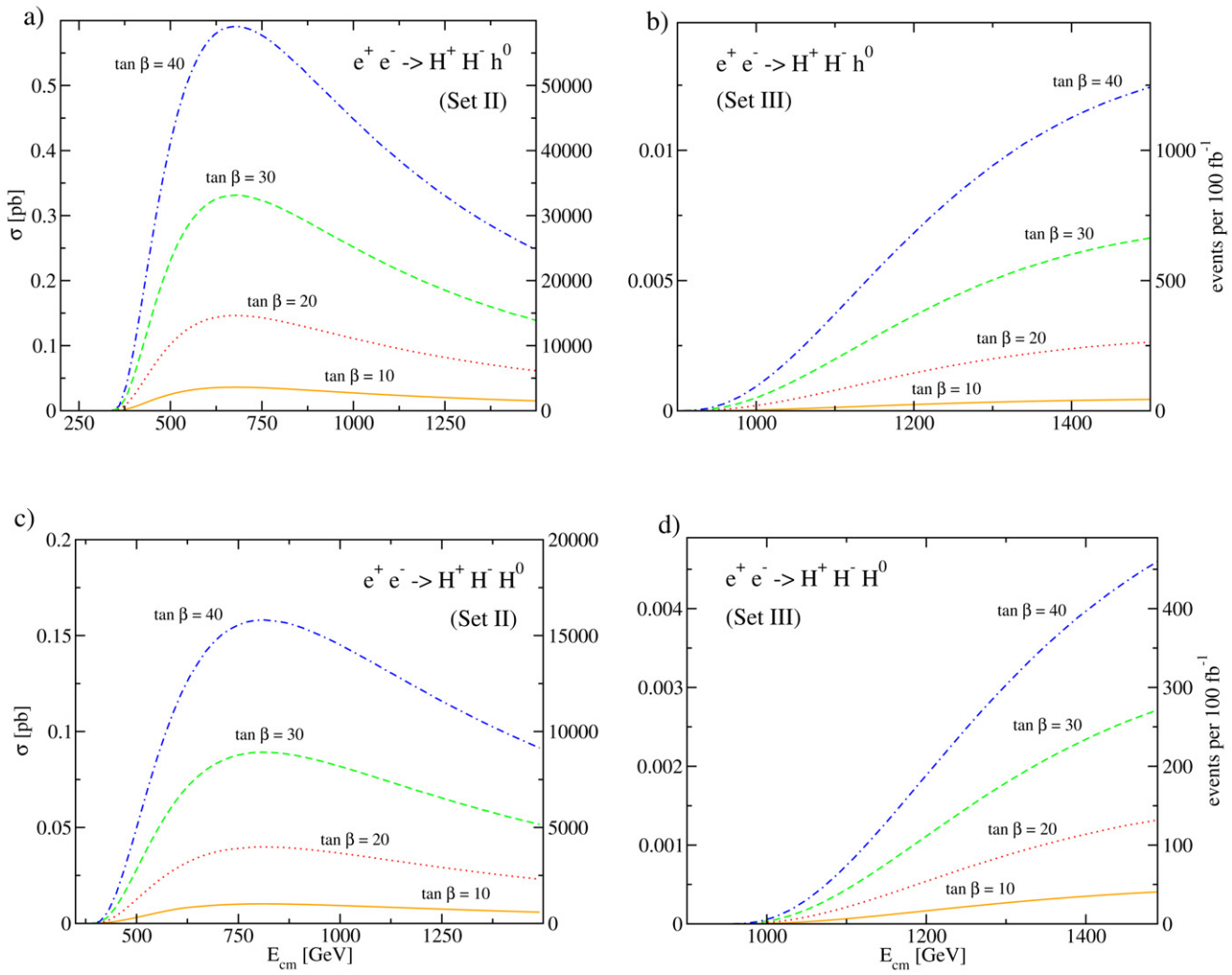

Fig. 3. Total cross-section σ (pb) and number of events per 100 fb^{-1} for the triple Higgs boson production processes $e^+e^- \to H^+H^-h^0$ and $e^+e^- \to H^+H^-H^0$ in the general 2HDM as a function of $\sqrt{s}$ and for different values of $\tan\beta$. In each case the label of the process and the choice (Set II or Set III) of Higgs boson masses used for the calculation is indicated, see Table 2.

For completeness, let us also mention that the corresponding values of the parameter λ_5 in Figs. 3 and 4 are around $\lambda_5 = 3$ for Set II and $\lambda_5 = 4$ for Set III.

To compare the 2HDM results with the corresponding supersymmetric values we have computed all the 3H production rates $\sigma(3H)$ in the framework of the MSSM. We have searched for the optimal regions of the MSSM parameter space where the largest allowed values for the cross-sections are obtained. Specifically, in Table 5 we provide the maximum value that $\sigma(3H)$ can achieve for each process and for two different values of the center-of-mass energy ($\sqrt{s} = 1$ TeV and 1.4 TeV) after scanning on (M_{A^0}, $\tan\beta$) for the fixed values of the MSSM parameter space quoted in Table 4. Again the latter determine the Higgs boson masses at the quantum level from the results of Ref. [20]. Let us notice from Table 5 that the channel $e^+e^- \to h^0h^0A^0$ has a cross-section that is substantially larger than the others, the reason being that it can pick up the resonant decay $H^0 \to h^0h^0$ whose branching ratio is non-negligible in these conditions [4]. As a consequence $\sigma(e^+e^- \to h^0h^0A^0)$ is of the order of an average 2H cross-section (cf. Table 3) times this branching ratio. This effect has been studied in detail by including the MSSM radiative corrections to the trilinear coupling, which turn out to be important in this region and are responsible for $\mathcal{B}(H^0 \to h^0h^0)$ being sizeable (of order 50%). As a result the cross-section can be $\mathcal{O}(10^{-3})$ pb, i.e. of a few fb. This situation is special in the MSSM, and an accurate evaluation of it depends on the specific choice of parameter values, see [4,7]. The great enhancement associated with it gives some hope for measuring this particular 3H channel in the MSSM.

In the general 2HDM, that resonant situation is not especially noticeable because the 3H channels are usually of the same order as the 2H ones, if not dominant. Therefore, barring that resonant process, in all the other cases the MSSM cross-sections for 3H production are very small, reaching maximum values of $\sigma \sim 10^{-6}$ pb at most for the leading processes indicated in Table 5. The remaining 3H channels in the MSSM, namely those with final states $H^+H^-A^0$, $H^0H^0A^0$ and $A^0A^0A^0$, furnish maximum cross-sections in the range (10^{-7}–10^{-8}) pb. As a matter of fact, we can assert that most of the 3H cross-

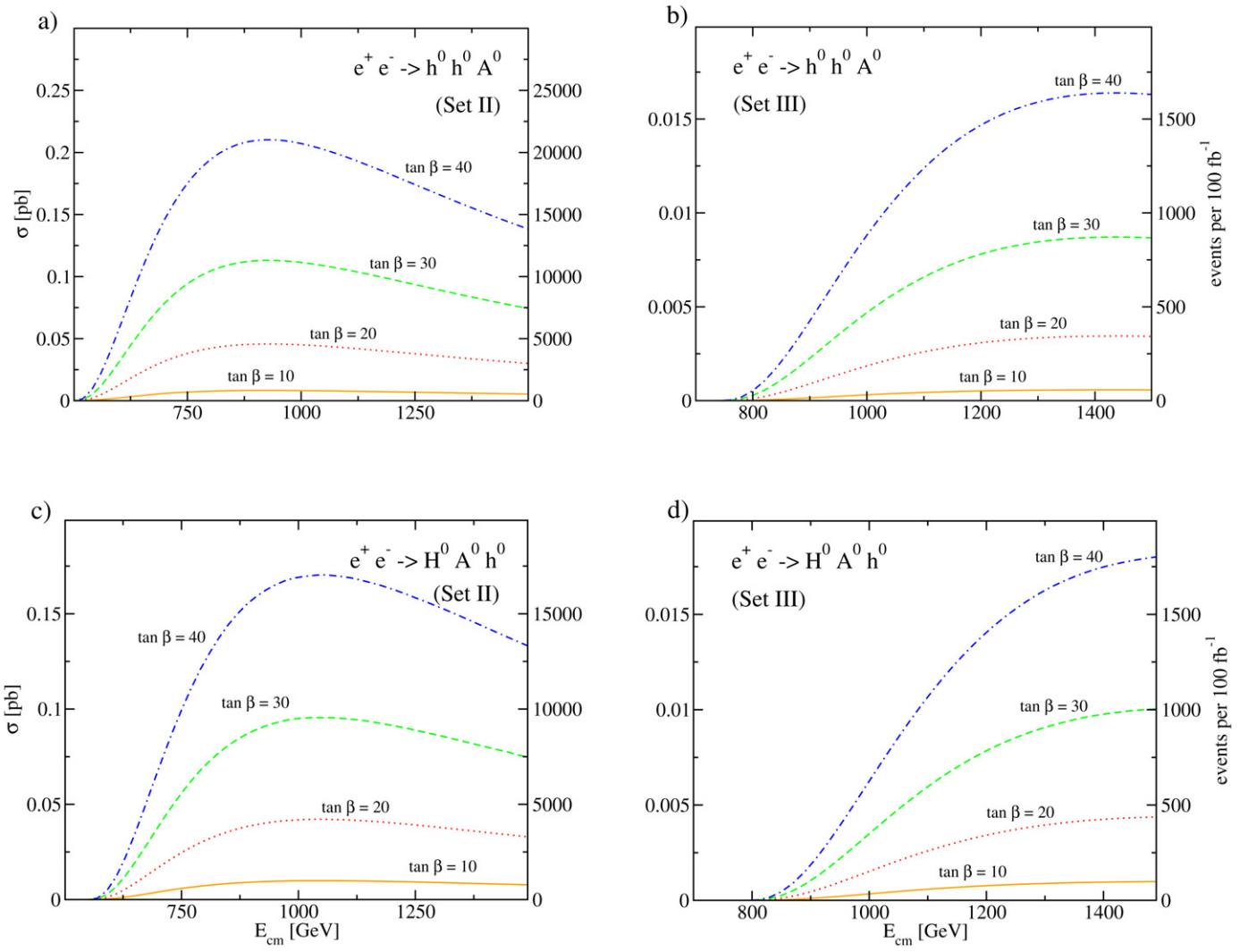

Fig. 4. As in Fig. 3, but for processes $e^+e^- \to h^0h^0A^0$ and $e^+e^- \to H^0A^0h^0$.

Table 5
Maximum cross-sections (in pb) for the leading 3H processes within the MSSM at two values of the center of mass energy, $\sqrt{s} = 1$ TeV and 1.4 TeV. The maximizing values of M_{A^0} and $\tan\beta$ are also indicated and are (approximately) the same at the two energies. The 3H processes non-included are even more suppressed

	$\sigma_{\max}$ (1 TeV)	$\sigma_{\max}$ (1.4 TeV)	M_{A^0} (GeV)	$\tan\beta$
$e^+e^- \to H^+H^-h^0$	5.6×10^{-6}	3.6×10^{-6}	135	3
$e^+e^- \to H^+H^-H^0$	1.5×10^{-6}	9.1×10^{-7}	100	30
$e^+e^- \to h^0h^0A^0$	1.2×10^{-3}	7.3×10^{-4}	200	2.5
$e^+e^- \to H^0A^0h^0$	2.0×10^{-6}	1.4×10^{-6}	100	5.5

sections in the MSSM are of the same order as—if not smaller than—the tiny rates for the one-loop 2H processes $e^+e^- \to hh$ (with two identical Higgs particles in the final state) mentioned in the beginning of this section. In short, we conclude that the maximum MSSM cross-sections for 3H production are typically 10^4 times smaller than the corresponding maximum 2HDM values (even if taking Set III of Higgs boson masses). In the light of these results it becomes clear that the triple Higgs boson channels are in general much more promising in the 2HDM (both in types I and II) than in the MSSM, and can be fully competitive with the 2H ones.

4. Discussion and conclusions

We have devoted this work to the study of the triple Higgs boson final states (1.2) produced in a linear e^+e^- collider. We have computed the cross-sections for these processes both in the Minimal Supersymmetric Standard Model (MSSM) and in the general Two-Higgs-Doublet Model (2HDM). The results are in principle independent of which kind of 2HDM model is used, type I or type II, because the 3H processes (1.2) are not sensitive to the Higgs boson interactions with fermions. However, radiative B-meson decays (characterized by the $b \to s\gamma$ subprocess) place an important constraint on the lower value of the charged Higgs boson mass of type II models, namely $M_{H^\pm} \gtrsim 350$ GeV, and this fact is what actually puts an upper bound to the 3H cross-sections for type II models. We have found that within the type I model the triple Higgs boson cross-sections may comfortably reach 0.1 pb for $\tan\beta$ sufficiently

large ($\tan\beta \gtrsim 20$) or small ($\tan\beta < 0.1$)[3]; actually, in certain regions of parameter space they can be pushed up to 1 pb, the most favorable process being $e^+e^- \to H^+H^-h^0$. This is also the preferred channel for type II models, but due to the aforesaid charged Higgs boson mass bound the maximum cross-section is roughly 10 times smaller, i.e. of order of 0.01 pb. The number of events is nonetheless of order 10^3 per 100 fb^{-1} of integrated luminosity, and in both cases the cross-section is far larger than in the MSSM. For example, the maximum cross-section for $e^+e^- \to H^+H^-h^0$ in the MSSM is at most of order 10^{-6} pb, i.e. around 10^4 times smaller than the corresponding one in general type II Higgs boson models (of which the MSSM Higgs sector is a very particular case).

Another remarkable fact that we would like to emphasize is that for the general 2HDM models the maximum cross-sections for the 3H processes (1.2) are comparable or even larger than the maximum cross-sections for the 2H processes (1.1). Notice that, in spite of having one more particle in the final state, the mechanism of 3H production is peculiar in that it involves certain trilinear Higgs boson couplings that can be enhanced in the general 2HDM, e.g. at large $\tan\beta > 20$. This enhancement is impossible in the MSSM, due to the purely gauge nature of the Higgs boson self-interactions in this model which is enforced by the invariance of the potential under supersymmetric transformations. Incidentally, the 2H cross-sections for the unconstrained 2HDM models are of the same order as the 2H cross-sections in the MSSM. In view of these facts, we expect that the 3H production channels in the general 2HDM could be competitive at the ILC and provide a direct window for uncovering the structure of the Higgs potential.

We have found that the regions of parameter space with the largest possible values of $\tan\beta$ and relatively small α turn out to maximize the 3H cross-sections. For type II models (characterized by a heavier spectrum of Higgs boson masses) this means that the dominant decay modes for each of the Higgs bosons in a typical final state like $H^+H^-h^0$ will be into heavy quarks. Specifically, the neutral Higgs boson will decay as $h^0 \to b\bar{b}$ and the charged ones as $H^+ \to t\bar{b}$ and $H^- \to \bar{t}b$. The last two decays assume of course $M_{H^\pm} > m_t + m_b$, which is indeed always the case due to the $b \to s\gamma$ constraint for type II models. In this region of parameter space, the alternate Higgs boson decays into gauge bosons (such as $h^0 \to W^+W^-$, ZZ) are not dominant—in contradistinction to the SM Higgs boson decays. Other modes like $H^\pm \to W^\pm h^0$, even if kinematically open, are suppressed by trigonometric factors in the coupling strength, viz. $\cos(\beta-\alpha) \to 0$ in the favorable regions for 3H production. In this region, typically 2/3 of the Higgs boson decays contribute to the 6 heavy-quark jet final states, the rate being larger the larger is $\tan\beta$. In practice we would expect seeing a 4-prong final state made out of b- and $\bar{b}$-jets together with a $t\bar{t}$ system decaying in the conventional manner. This configuration represents the characteristic signature of the 3H processes under consideration. Although a dedicated experimental study would be necessary to assess its real possibilities, we expect that in the extremely clean context of the ILC this signature could hardly be missed and, if effectively found, it would represent a strong hint of (non-supersymmetric) Higgs boson physics beyond the SM.

[3] The neighborhood $\tan\beta \lesssim 0.1$ borders the perturbativity limit of the top quark Yukawa coupling, and thus the region $\tan\beta < 1$ becomes rapidly excluded.

Acknowledgements

This work has been supported in part by the EU project RTN MRTN-CT-2006-035505 Heptools; G.F. thanks an ESR position of this network, and the hospitality of the Departament ECM, Universitat de Barcelona where this work was carried out. D.L.V. has been supported by the MEC FPU grant AP2006-00357; J.G. and J.S. are also supported by MEC and FEDER under project 2004-04582-C02-01 and by DURSI Generalitat de Catalunya under project 2005SGR00564.

References

[1] H.P. Nilles, Phys. Rep. 110 (1984) 1;
H.E. Haber, G.L. Kane, Phys. Rep. 117 (1985) 75.
[2] J.F. Gunion, H.E. Haber, G.L. Kane, S. Dawson, The Higgs Hunter's Guide, Addison–Wesley, Menlo-Park, 1990.
[3] A. Djouadi, H.E. Haber, P.M. Zerwas, Z. Phys. C 57 (1993) 569.
[4] A. Djouadi, H.E. Haber, P.M. Zerwas, Phys. Lett. B 375 (1996) 203, hep-ph/9602234;
A. Djouadi, V. Driesen, W. Hollik, J. Rosiek, Nucl. Phys. B 491 (1997) 68, hep-ph/9609420.
[5] J.L. Feng, T. Moroi, Phys. Rev. D 56 (1997) 5962, hep-ph/9612333.
[6] V. Driesen, W. Hollik, J. Rosiek, Z. Phys. C 7 (1996) 259, hep-ph/9512441;
E. Coniavitis, A. Ferrari, Phys. Rev. D 75 (2007) 015004;
S. Heinemeyer, Int. J. Mod. Phys. 21 (2006) 2659.
[7] A. Djouadi, W. Kilian, M. Muhlleitner, P.M. Zerwas, Eur. Phys. J. C 10 (1999) 27, hep-ph/9903229;
For tree-level double Higgs production processes, see e.g. the exhaustive overview by M. Muhlleitner, hep-ph/0008127.
[8] P. Osland, P.N. Pandita, Phys. Rev. D 59 (1998) 055013;
D.J. Miller, S. Moretti, Eur. Phys. J. C 13 (2000) 459;
F. Boudjema, A. Semenov, Phys. Rev. D 66 (2002) 095007.
[9] G. Weiglein, Phys. Rep. 426 (2006) 47, hep-ph/0410364.
[10] J. Guasch, W. Hollik, A. Kraft, Nucl. Phys. B 596 (2001) 66.
[11] A. Djouadi, W. Kilian, M. Muhlleitner, P.M. Zerwas, Eur. Phys. J. C 10 (1999) 45, hep-ph/9904287;
T. Binoth, S. Karg, N. Kauer, R. Ruckl, Phys. Rev. D 74 (2006) 113008, hep-ph/0608057.
[12] G. Ferrera, J. Guasch, D. López-Val, J. Solà, in preparation.
[13] S. Béjar, J. Guasch, J. Solà, Nucl. Phys. B 600 (2001) 21, hep-ph/001091;
S. Béjar, J. Guasch, J. Solà, Nucl. Phys. B 675 (2003) 270, hep-ph/0307144;
S. Béjar, PhD Thesis, hep-th/0606138.
[14] M.B. Einhorn, D.R.T. Jones, M.J.G. Veltman, Nucl. Phys. B 191 (1981) 146.
[15] W.M. Yao, et al., Particle Data Group, J. Phys. G 33 (2006) 1.
[16] R. Barbieri, L. Maiani, Nucl. Phys. B 224 (1983) 32.
[17] P. Gambino, M. Misiak, Nucl. Phys. B 611 (2001) 338, hep-ph/0104034;
M. Ciuchini, G. Degrassi, P. Gambino, G.F. Giudice, Nucl. Phys. B 527 (1998) 21, hep-ph/9710335;
F.M. Borzumati, C. Greub, Phys. Rev. D 58 (1998) 074004, hep-ph/9802391;
F.M. Borzumati, C. Greub, Phys. Rev. D 59 (1999) 057501, hep-ph/9809438, Addendum.

[18] S. Kanemura, T. Kubota, E. Takasugi, Phys. Lett. B 313 (1993) 155, hep-ph/9303263;
A.G. Akeroyd, A. Arhrib, E.-M. Naimi, Phys. Lett. B 490 (2000) 119, hep-ph/0006035;
J. Horejsi, M. Kladiva, Eur. Phys. J. C 46 (2006) 81, hep-ph/0510154.
[19] T. Hahn, FeynArts 3.2, FormCalc and LoopTools user's guides, available from http://www.feynarts.de;
T. Hahn, Comput. Phys. Commun. 168 (2005) 78, hep-ph/0404043.
[20] S. Heinemeyer, W. Hollik, G. Weiglein, Phys. Lett. B 455 (1999) 179, hep-ph/9903404.
[21] W. Hollik, S. Peñaranda, Eur. Phys. J. C 23 (2002) 163, hep-ph/0108245;
A. Dobado, M.J. Herrero, W. Hollik, S. Peñaranda, Phys. Rev. D 66 (2002) 095016, hep-ph/0208014;
A. Dobado, M.J. Herrero, W. Hollik, S. Peñaranda, hep-ph/0210315.
[22] S. Kanemura, Y. Okada, E. Senaha, Phys. Lett. B 606 (2005) 361, hep-ph/0411354;
S. Kanemura, Y. Okada, E. Senaha, hep-ph/0507259.